
SpaceMind++: Toward Allocentric Cognitive Maps for Spatially Grounded Video MLLMs

Bo Gu^{1†}, Zhikang Zhang^{2†}, Zizhuang Wei², Zhenyuan Chen²
Lingyun Li^{2*}, Zhuoyi Song^{3,1*}

¹Fudan University ²Huawei ³Shenzhen Loop Area Institute
† Equal contribution * Corresponding author

Abstract

Recent multimodal large language models (MLLMs) have made remarkable progress in visual understanding and language-based reasoning, yet they lack a persistent world-centered representation for spatially consistent reasoning in 3D environments. Inspired by the mammalian dual-stream system, where semantic and spatial cues are processed separately and integrated into an allocentric cognitive map, we propose *SpaceMind++*, a video MLLM architecture that explicitly builds a voxelized cognitive map from RGB videos. This map reorganizes fragmented egocentric observations into a shared 3D metric representation, enabling the model to preserve object permanence and spatial topology across changing viewpoints. To make this allocentric representation usable by a pretrained video MLLM without disrupting its native visual-token interface, we introduce Coordinate-Guided Deep Iterative Fusion, a new mechanism that relays map-level spatial knowledge back into the original 2D visual features. This fusion is explicitly guided by coordinate embeddings and 3D Rotary Positional Encoding, which ground semantic interactions in metric 3D space, resembling the entorhinal binding of sensory features to metric space. Extensive experiments show that *SpaceMind++* achieves new **state-of-the-art** performance on VSI-Bench. Furthermore, it demonstrates superior **out-of-distribution generalization** on SPBench, SITE-Bench, and SPAR-Bench, underscoring its robustness in unseen 3D environments.

1 Introduction

Spatial intelligence requires models to reason about the 3D structure of environments beyond isolated visual observations. Despite recent advances that have endowed Multimodal Large Language Models (MLLMs) with strong visual understanding and reasoning capabilities[3, 29, 32, 75], a fundamental gap persists between language-level reasoning and 3D spatial organization[57, 70]. This disconnect limits the ability of MLLMs to ground their predictions in physical space, leading to unstable spatial reasoning, such as inconsistent distance estimation and object-level hallucinations[65]. This limitation stems from a lack of spatial constancy: visual observations are egocentric, partial, and transient, with viewpoint-dependent distances, occlusions, and fragmented frame-level evidence of the underlying 3D scene.

Recent efforts to build 3D-aware MLLMs attempt to address this issue by incorporating feed-forward geometry encoders alongside general-purpose visual encoders. These methods commonly fuse 2D visual features and 3D geometric cues through MLPs[61], cross-attention[13], or camera-guided integration[72]. However, they largely treat geometry as an auxiliary modality aligned with egocentric visual tokens, enhancing spatial cues only locally without forming an explicit and persistent 3D structure. Rather, reliable spatial intelligence requires more than extracting geometric cues from

individual observations; it requires a stable world-centered representation that preserves object permanence, metric consistency, and global scene layout across changing viewpoints.

Human spatial cognition offers a blueprint for spatially grounded reasoning. Neuroscience studies highlight two key mechanisms for spatial awareness: the dual visual stream [18, 52] and the cognitive map [22, 38, 51]. The former separates visual processing into ventral “what” and dorsal “where” pathways, while the latter provides an allocentric representation for reasoning about spatial relationships beyond the current field of view. Although cognitive maps have inspired computational models such as the Tolman-Eichenbaum Machine [58–60] and visual-language navigation systems [20, 45], their use as an architectural principle for large-scale MLLMs remains under-explored.

Inspired by principles of human spatial cognition, we present **SpaceMind++**, a video MLLM that introduces an allocentric cognitive map as a first-class architectural component for spatial reasoning. In contrast to prior 3D-aware MLLMs that treat 3D geometry as an auxiliary feature stream, SpaceMind++ projects frame-level 2D semantic features into a voxelized map organized in 3D space. This transformation converts fragmented egocentric observations into a structured world-centered representation, allowing the model to maintain spatial topology across viewpoints.

To make this map useful for language reasoning, we further introduce **Coordinate-Guided Deep Iterative Fusion (CDIF)**, which relays spatial knowledge from the map back to the original visual tokens through iterative map self-attention and map-to-visual cross-attention. The LLM therefore receives geometry-enhanced visual tokens while preserving the pretrained visual-language interface. A key requirement for such fusion is that semantic interactions must be governed by metric 3D relationships rather than by arbitrary sequence order. Inspired by hippocampal–entorhinal spatial coding, which supports metric and allocentric representations of space [22, 43, 44], we make attention coordinate-aware by injecting explicit 3D coordinate embeddings and applying 3D Continuous Rotary Position Embeddings. This design binds visual semantics to spatial locations during both attention steps, enabling SpaceMind++ to reason over object relations within a 3D metric structure. Experiments on VSIBench and other benchmarks demonstrate that SpaceMind++ achieves state-of-the-art performance in a wide range of visual-based spatial understanding and reasoning tasks.

In summary, our main contributions are:

- We introduce a brain-inspired design perspective for spatially grounded video MLLMs, drawing motivation from the mammalian dual visual stream and cognitive map to separate semantic recognition, spatial localization, and allocentric scene organization.
- We propose SpaceMind++, a novel video MLLM architecture that builds a voxelized allocentric cognitive map from RGB videos, effectively preserving spatial topology and object permanence across diverse viewpoints.
- We introduce Coordinate-Guided Deep Iterative Fusion (CDIF), a coordinate-aware mechanism that performs iterative map reasoning and map-to-visual reading with explicit 3D coordinate embeddings and 3D RoPE, while keeping the pretrained MLLM interface intact.
- We curate SpaceMind-900K for spatial instruction tuning and validate SpaceMind++ across multiple benchmarks, achieving new state-of-the-art performance on VSI-Bench and strong generalization on SPBench, SITE-Bench, and SPAR-Bench.

2 Related Work

2.1 Spatial Reasoning in Multimodal Large Language Models

Multimodal large language models (MLLMs) have achieved strong progress in visual question answering, image captioning, and video understanding[1, 2, 8, 31, 32, 42, 75], yet they remain unreliable on spatially grounded tasks such as metric estimation, spatial relationship judgment, and navigation-oriented reasoning[49, 65, 69]. Aiming to solve this problem, existing spatial MLLMs can be broadly grouped into two lines. One line introduces explicit 3D inputs, including point clouds[16, 23, 36] and depth maps[5, 10, 73], and aligns these structured scene representations with language models. Although effective when high-quality geometry is available, these methods often rely on reconstruction pipelines, limiting their scalability to unconstrained RGB videos. Another line improves RGB-based spatial reasoning by augmenting VLMs with 3D geometry encoders or internal spatial representations, as explored in Spatial-MLLM[61], VLM-3R[13] and SpaceMind[72]. These

approaches demonstrate the value of geometric priors, but typically integrate spatial information through token-level fusion. Such designs enhance local spatial cues but do not explicitly reorganize observations into a persistent world-centered structure. Our work instead treats 3D geometry as the organizing substrate for constructing an allocentric cognitive map, enabling more stable spatial reasoning across changing viewpoints.

2.2 Feed-forward Visual Geometry for 3D Scene Understanding

Classical 3D reconstruction pipelines, such as Structure-from-Motion [46] and Multi-View Stereo [47, 53, 68], recover camera poses and dense geometry from images. However, their reliance on multi-stage optimization and sufficient view overlap makes them difficult to integrate into end-to-end multimodal reasoning systems. Recent feed-forward visual geometry models, including DUS3R[56], MAST3R[28], CUT3R[55], and VGGT[54], alleviate this limitation by directly predicting dense correspondences, point maps, depth, and camera parameters from RGB images or short sequences. These models provide scalable geometric priors for in-the-wild inputs and have been increasingly adopted by geometry-aware MLLMs[13, 61]. Nevertheless, their outputs are primarily designed for reconstruction rather than language-conditioned spatial reasoning, and existing MLLMs typically use them as auxiliary token-level features through projection layers or cross-attention[13, 61]. In contrast, our work converts feed-forward geometry into a voxelized cognitive map, where semantic features are aggregated in a persistent 3D metric space to support cross-view and allocentric spatial reasoning.

2.3 Brain-inspired spatial reasoning for MLLM

Brain-inspired reasoning has recently been explored as a way to improve the spatial reasoning of MLLMs. At a high level, cognitive maps offer a useful abstraction for organizing local observations into structured environmental representations [12, 27, 71]. However, most existing MLLM studies adopt this idea only as an auxiliary reasoning scaffold. For example, Thinking-in-Space shows that a lightweight grid-based cognitive map can improve MLLMs’ spatial layout understanding [65]. SpaceR encourages 2D object-layout map imagination during reinforcement learning [41], while Video2Layout replaces coarse grid maps with metric-grounded BEV layouts for finer spatial computation [26]. These methods highlight the value of spatial layouts, but their representations remain largely planar and object-level abstractions.

Another line of work develops 3D-aware representations for spatial reasoning. LLaVA-3D constructs 3D patches by injecting 3D position embeddings into 2D visual patches [74], while 3DLLM-Mem introduces long-term spatiotemporal memory to retrieve task-relevant information across extended trajectories [25]. More recently, Map2Thought constructs an object-centric Metric-CogMap for deterministic Cog-CoT reasoning[17], while Cog3DMap builds a compact 3D memory from multi-view images and directly feeds map tokens into the MLLM instead of visual tokens[21]. In contrast, SpaceMind++ does not treat the map as a final object-level reasoning layout or as a replacement for visual tokens. Instead, it uses the map as an intermediate coordinate-grounded neural workspace and returns spatial knowledge to the original visual-token interface.

3 Method

3.1 Overall Architecture

The goal of SpaceMind++ is to empower Multimodal Large Language Models (MLLMs) with a 3D cognitive structure, enabling precise spatial reasoning in physical environments. Given a sequence of RGB video frames $\mathcal{S} = \{I_i\}_{i=1}^N$, $I_i \in \mathbb{R}^{3 \times H \times W}$ and a textual prompt T , our model performs a multi-stage transformation that grounds language reasoning in a structured 3D metric space. SpaceMind++ follows the brain-inspired dual-stream design (left in Figure 1) and instantiates it as a three-stage video MLLM architecture (right in Figure 1): dual-stream feature extraction, allocentric cognitive map construction, and map-to-visual fusion.

Dual-stream feature extraction. Inspired by the biological dual-pathway process, we first decompose the input video into semantic and geometric streams.

Ventral stream A pretrained 2D visual encoder E_v (InternViT) extracts semantic tokens $f_v \in \mathbb{R}^{N \times M_v \times D_v}$ from the video frames, capturing *what* is present in the scene.

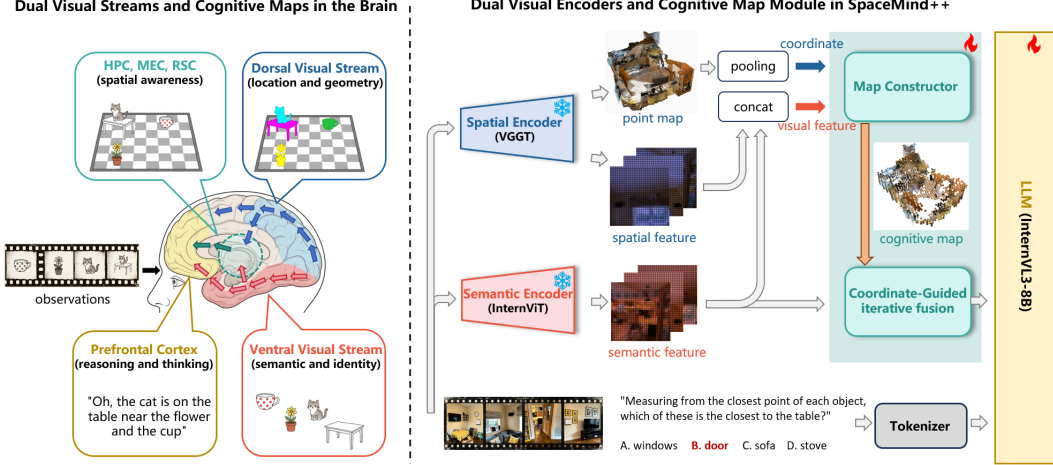


Figure 1: **Left:** biological motivation. Mammalian spatial cognition separates semantic identity and geometric localization through ventral (red area) and dorsal visual streams (red area), and integrates them into an allocentric cognitive map (cyan area) for spatial awareness and reasoning. **Right:** model architecture. SpaceMind++ extracts semantic and spatial features from video, organizes them into a voxelized allocentric cognitive map, and uses CDIF to relay map-level spatial knowledge back to visual tokens before language decoding (downward yellow arrow).

Dorsal stream Simultaneously, a geometry-aware spatial encoder E_s (e.g., VGGT[54]) processes the same input to produce the geometric latent features $f_s \in \mathbb{R}^{N \times M_v \times D_s}$, per-pixel 3D coordinates $P \in \mathbb{R}^{N \times H \times W \times 3}$ and confidence scores $C \in \mathbb{R}^{N \times H \times W \times 1}$, representing *where* objects are located.

$$f_v = E_v(\mathcal{S}), \quad \{f_s, P, C\} = E_s(\mathcal{S}). \quad (1)$$

Allocentric cognitive map fusion. The core of SpaceMind++ is the Cognitive Map module, which integrates the dual-stream features in an explicit 3D space. It scatters egocentric visual tokens into a unified voxel grid according to their 3D coordinates, producing an allocentric cognitive map \mathcal{M} :

$$\mathcal{M} = \text{Voxelize}(f_v, f_s, P), \quad f_{\text{fused}} = \mathcal{F}(f_v, \mathcal{M}, P). \quad (2)$$

To make the map accessible to the pretrained LLM without changing its visual-token interface, \mathcal{F} alternates between *spatial reasoning* over map tokens and *map reading* from map tokens back to visual tokens (the coordinate-guided iterative fusion module in Figure 1), progressively injecting 3D spatial knowledge into the original visual stream as f_{fused} .

Language decoding. The resulting geometry-enhanced visual tokens are fed into the LLM backbone G together with the text prompt T to generate response R .

3.2 Allocentric Cognitive Map Construction

As illustrated in the left part of Figure 2, the map constructor converts patch-level visual features and 3D coordinates into a compact voxelized cognitive map through coordinate quantization, topology-preserving aggregation, and stochastic sampling.

3.2.1 Dynamic Coordinate Quantization

We first align the dense geometric outputs of the spatial encoder with the patch-level visual tokens. Specifically, the dense point map and confidence map are average-pooled to the visual-token resolution, producing patch-aligned coordinates $P \in \mathbb{R}^{L \times 3}$ and confidence scores $C \in \mathbb{R}^{L \times 1}$, where $L = N \times M_v$. To reduce the effect of noisy geometry, we retain only high-confidence coordinates and compute a dynamic scene center $\mathbf{c} \in \mathbb{R}^3$ as their centroid:

$$\mathbf{c} = \frac{1}{|\mathcal{V}_{\text{valid}}|} \sum_{i \in \mathcal{V}_{\text{valid}}} P_i, \quad \text{where } \mathcal{V}_{\text{valid}} = \{i \mid C_i > \tau_{\text{conf}}\}. \quad (3)$$

Here, τ_{conf} is the confidence threshold. We then recenter each coordinate by the dynamic scene center, $\tilde{P}_i = P_i - \mathbf{c}$, and discretize the recentered 3D space into a voxel grid with extent D (we set D as 100 for all experiments) and scale-free resolution r . Since the spatial encoder predicts geometry in a relative metric space, r is defined on this normalized scale rather than in absolute physical units. The continuous coordinates are quantized into integer voxel indices $\mathbf{u}_i = (u_{x,i}, u_{y,i}, u_{z,i}) \in \mathbb{Z}^3$:

$$\mathbf{u}_i = \left\lfloor \frac{\tilde{P}_i}{r} \right\rfloor + \frac{D}{2}. \quad (4)$$

This step corresponds to the feature voxelization panel in Figure 2, where continuous 3D coordinates are mapped into discrete voxel indices so that tokens from nearby locations can be grouped together. After that, we convert each 3D voxel index into a unique 1D spatial hash key h_i for efficient grouping:

$$h_i = u_{x,i}D^2 + u_{y,i}D + u_{z,i}. \quad (5)$$

Because mapping 3D spatial coordinates into a 1D index array strictly requires a predefined boundary limit, tokens whose computed 3D indices fall outside the grid extent $[0, D - 1]^3$ are truncated.

3.2.2 Topology-Preserving Feature Aggregation

In video streams, the same physical region may be observed repeatedly, causing substantial token redundancy. We therefore use voxelization as a geometry-aware bottleneck and group tokens by their 1D spatial hash keys h . Let $\mathcal{H}_j = \{i \mid h_i = j\}$ denote the set of tokens assigned to the j -th voxel.

As shown in Figure 2, tokens within each voxel are aggregated into one compact map token after filtering inconsistent observations. We first compute a voxel centroid $\boldsymbol{\mu}_j$ by averaging the concatenated features $x_i = [f_{v,i}; f_{s,i}]$ in the bin, which represents the consensus semantic-geometric state of that physical region. We then remove outlier observations whose cosine similarity to $\boldsymbol{\mu}_j$ is below τ_{sim} :

$$\tilde{\mathcal{H}}_j = \left\{ i \in \mathcal{H}_j \mid \frac{x_i \cdot \boldsymbol{\mu}_j}{\|x_i\| \|\boldsymbol{\mu}_j\|} > \tau_{\text{sim}} \right\}, \quad \boldsymbol{\mu}_j = \frac{1}{|\mathcal{H}_j|} \sum_{i \in \mathcal{H}_j} x_i. \quad (6)$$

The final representation for the j -th voxel is obtained by applying scatter-mean pooling over the refined set $\tilde{\mathcal{H}}_j$:

$$\mathbf{v}_j = \frac{1}{M_j} \sum_{i \in \tilde{\mathcal{H}}_j} x_i, \quad \mathbf{p}_j = \frac{1}{M_j} \sum_{i \in \tilde{\mathcal{H}}_j} \tilde{P}_i, \quad t_j = \min_{i \in \tilde{\mathcal{H}}_j} t_i, \quad M_j = |\tilde{\mathcal{H}}_j|. \quad (7)$$

Here, \mathbf{v}_j , \mathbf{p}_j , and t_j denote the voxel feature, spatial coordinate, and first-observed timestamp of the j -th voxel, respectively. By retaining the minimum timestamp among all assigned tokens, each voxel records when its corresponding physical region first appears in the video, providing a lightweight cue for appearance-order reasoning.

3.2.3 Global Stochastic Sampling for Scale Invariance

For large scenes, voxelization can yield dense maps. When the number of voxels M exceeds M_{max} , we uniformly sample M_{max} valid voxels instead of truncating the sequence, reducing redundancy while preserving the global spatial layout. We set $M_{\text{max}} = 5000$ in all experiments.

3.3 Coordinate-Guided Deep Iterative Fusion

After constructing the voxelized cognitive map, SpaceMind++ uses Coordinate-Guided Deep Iterative Fusion (CDIF) to transfer map-level spatial knowledge back to visual tokens while preserving the original visual-token interface. As shown in Figure 2, CDIF consists of L layers that alternate between Map Reasoning and Map Reading.

3.3.1 Map Reasoning via Self-Attention

Within each fusion layer l , CDIF first performs intra-map self-attention to propagate semantic and geometric information across voxels. We encode each voxel coordinate \mathbf{p}_j with an MLP and add it

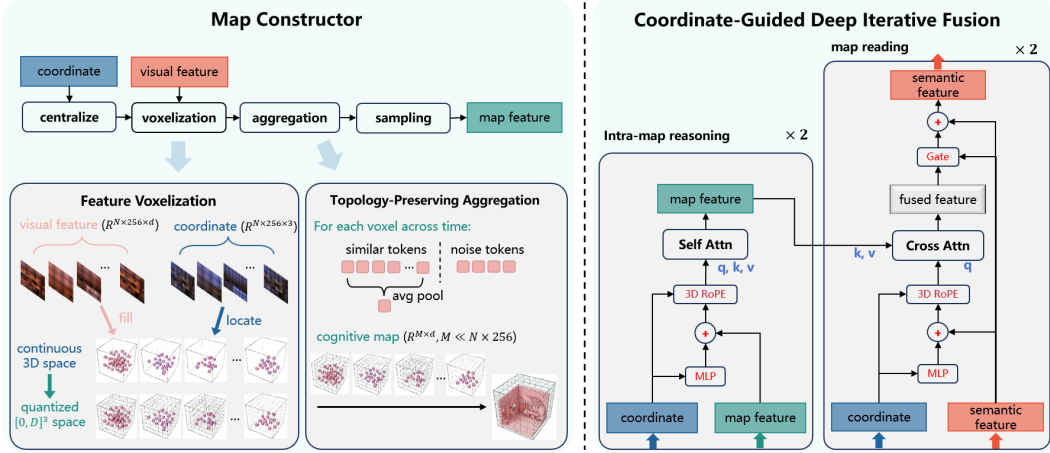


Figure 2: Detailed components of SpaceMind++. The map constructor transforms patch-level visual features and 3D coordinates into a voxelized cognitive map. CDIF then alternates between intra-map reasoning and map reading to inject spatial knowledge back into semantic tokens. Both stages are guided by coordinate embeddings and 3D RoPE to preserve metric 3D relationships.

to the voxel feature $\mathbf{v}_j^{(l)}$, then apply 3D Continuous Rotary Positional Embedding (3D RoPE) [50] to make the queries and keys coordinate-aware. This enables attention to model relative spatial relationships in metric 3D space:

$$\tilde{\mathbf{v}}_j^{(l)} = \mathbf{v}_j^{(l)} + \text{MLP}(\mathbf{p}_j), \quad \hat{\mathbf{q}}_j^{(l)}, \hat{\mathbf{k}}_j^{(l)} = \text{RoPE}(\text{Linear}(\tilde{\mathbf{v}}_j^{(l)}), \mathbf{p}_j). \quad (8)$$

The voxel map is then updated via self-attention:

$$\mathcal{V}^{(l+1)} = \text{SelfAttn}(\hat{\mathbf{Q}}, \hat{\mathbf{K}}, \mathbf{V}(\mathcal{V}^{(l)})). \quad (9)$$

This step enables the cognitive map to perform global geometric inference, such as modeling object-to-object spatial relationships, within a unified 3D coordinate frame.

3.3.2 Map Reading via Semantic-Aware Gated Attention

After the cognitive map is refined, each 2D visual token reads spatial context from the map. For a visual token $\mathbf{f}_{v,i}^{(l)}$ with 3D coordinate \mathbf{p}_i , we first inject its coordinate information through an MLP-based embedding. The coordinate-enhanced token is then projected into query and key modulated by 3D RoPE, making the map-reading attention aware of its metric location:

$$\tilde{\mathbf{f}}_{v,i}^{(l)} = \mathbf{f}_{v,i}^{(l)} + \text{MLP}(\mathbf{p}_i), \quad \mathbf{q}_i^{(l)} = \text{RoPE}(\text{Linear}(\tilde{\mathbf{f}}_{v,i}^{(l)}), \mathbf{p}_i). \quad (10)$$

The model then performs cross-attention over the refined voxel map $\mathcal{V}^{(l+1)}$ to retrieve the fused spatial feature $\mathbf{f}_{\text{fused},i}^{(l)}$:

$$\mathbf{f}_{\text{fused},i}^{(l)} = \text{CrossAttn}(\mathbf{q}_i^{(l)}, \mathbf{K}(\mathcal{V}^{(l+1)}), \mathbf{V}(\mathcal{V}^{(l+1)})). \quad (11)$$

Gated information integration. To prevent the visual stream from absorbing irrelevant geometric background, we introduce a visual-driven gating mechanism. Instead of unconditionally integrating all spatial information, the model uses the semantic content of the visual tokens to control the reading intensity. The gate $\mathbf{g}_i^{(l)}$ is computed solely from the visual feature:

$$\mathbf{g}_i^{(l)} = \sigma(\text{MLP}(\mathbf{f}_{v,i}^{(l)})). \quad (12)$$

The final updated visual representation is then formulated as:

$$\mathbf{f}_{v,i}^{(l+1)} = \mathbf{f}_{v,i}^{(l)} + \mathbf{g}_i^{(l)} \odot \text{FFN}(\mathbf{f}_{\text{fused},i}^{(l)}). \quad (13)$$

This design ensures that the 2D visual stream remains the primary carrier of semantic identity while selectively integrating 3D spatial knowledge only when the visual content, such as a specific object or landmark, requires geometric grounding for downstream reasoning.

Table 1: VSI-Bench evaluation. SpaceMind++ achieves the best overall performance and obtains the highest scores on most sub-tasks, demonstrating strong and balanced spatial reasoning ability.

Methods	Avg.	Numerical Question				Multiple-Choice Question			
		Obj. Cnt.	Abs. Dist.	Obj. Size	Room Size	Rel. Dist.	Rel. Dir.	Route Plan	Appr. Order
<i>Proprietary Models (API)</i>									
GPT-5 [48]	55.0	53.3	34.4	73.3	47.5	63.7	48.6	50.2	68.9
Gemini-3 Pro [19]	56.0	49.0	42.8	71.5	41.8	56.6	57.5	61.9	60.0
Grok-4 [63]	47.9	37.1	32.9	60.8	45.4	53.1	39.6	47.4	66.8
<i>Open-source VLMs</i>									
InternVL3-78B [75]	48.5	71.2	53.7	44.4	39.5	55.9	39.5	28.9	54.5
LLaVA-NeXT-Video-72B [33]	40.9	48.9	22.8	57.4	35.3	42.4	36.7	35.0	48.6
Qwen3VL-8B-Instruct [64]	57.9	<u>67.5</u>	<u>47.0</u>	76.3	61.9	58.0	50.9	35.0	66.3
LLaVA-OneVision-72B [29]	40.2	43.5	23.9	<u>57.6</u>	37.5	42.5	<u>39.9</u>	32.5	44.6
<i>Specialized Spatial Reasoning Models</i>									
Spatial-MLLM [61]	48.4	65.3	34.8	63.1	45.1	41.3	46.2	33.5	46.3
VST-7B [66]	60.6	72.0	44.4	74.3	68.3	59.7	55.8	44.9	65.2
VLM-3R [13]	60.9	70.2	49.4	69.2	67.1	65.4	80.5	45.4	40.1
SenseNova-SI-1.2 [6]	69.6	72.7	56.0	77.1	<u>75.7</u>	<u>70.4</u>	81.7	42.8	<u>79.9</u>
SpaceMind [72]	<u>70.2</u>	73.9	<u>61.5</u>	<u>77.6</u>	74.8	67.7	<u>88.6</u>	46.9	70.7
SpaceMind++ (Ours)	73.2	74.5	62.4	77.9	76.9	73.5	89.7	48.2	84.1

4 Implementation Details

Training data. We train SpaceMind++ on a spatial instruction-tuning corpus containing approximately 900k QA samples. The corpus integrates four 3D reasoning sources, including ViCA-322K[15], VLM-3R-data[13], SQA3D-train[35], and VSI-590K-Video[67]. As shown in Figure 3, the dataset covers a broad spectrum of spatial reasoning skills, including object counting, relative and absolute distance estimation, size estimation, object ordering, situated 3D perception, complex spatial reasoning, and route planning. This mixture encourages the model to learn both local metric grounding and global spatial consistency, which are essential for reasoning on an allocentric cognitive map.

Training setup. We use InternVL3-8B [75] as the base MLLM and keep both the ViT backbone and VGGT encoder frozen during training. We train the CDIF layers and the associated cross-modal projectors, while applying LoRA [24] to the language model with rank $r = 256$ and scaling factor $\alpha = 512$. The trainable parameters are optimized with AdamW [34] using a cosine annealing schedule and a peak learning rate of 2×10^{-5} . Training is conducted on 64 NVIDIA H200 GPUs for approximately 41 hours.

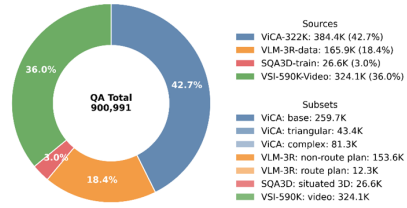
5 Evaluation

We evaluate SpaceMind++ on four spatial reasoning benchmarks. VSI-Bench is used as the primary benchmark for video-based spatial intelligence, while SPBench, SITE-Bench, and SPAR-Bench are used to assess generalization across multi-view and video spatial reasoning settings.

5.1 VSI-Bench

As shown in Table 1 and Figure 3, SpaceMind++ achieves a new state-of-the-art average score of 73.2, improving upon the strong SpaceMind baseline on VSI-Bench. Although SpaceMind and SenseNova-

Training Data Composition by Source



Training Data Composition by Task Type

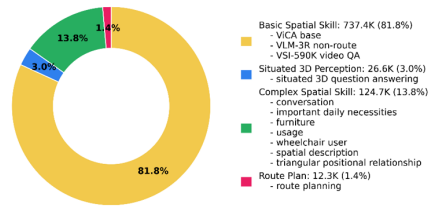


Figure 3: Statistics of the SpaceMind-900K datasets

Table 2: Generalization evaluation on SPBench and SITE-Bench. SpaceMind++ achieves strong out-of-domain performance, especially on multi-view SPBench and video-only SITE-Bench, demonstrating its advantage in cross-view and video spatial reasoning.

Methods	SPBench-SI			SPBench-MV			SPBench	SITE-Bench
	NQ	MCQ	Avg.	NQ	MCQ	Avg.		
<i>Proprietary Models</i>								
GPT-4o [40]	24.5	60.3	42.4	40.7	59.4	50.1	46.2	–
Gemini-2.0-Flash [11]	49.0	60.4	54.7	51.9	50.7	51.3	53.0	–
<i>Open-Source Models</i>								
InternVL-2.5-8B [7]	28.3	56.3	42.3	37.3	47.5	42.4	42.3	–
Kimi-VL-A3B [37]	25.7	44.9	35.3	23.3	57.6	40.5	37.9	–
LLaVA-OneVision-7B [29]	25.4	41.0	33.2	20.6	49.6	35.1	34.2	–
Qwen2.5-VL-7B [3]	36.3	60.5	48.4	28.9	49.8	39.3	43.9	53.7
<i>Spatial Reasoning Models</i>								
Video-R1 [14]	27.7	62.0	44.9	32.5	53.0	42.8	43.8	–
SpaceR-7B [41]	35.7	61.5	48.6	63.2	53.7	58.5	53.5	56.5
VILASR-7B [62]	36.6	63.7	50.2	56.2	59.6	57.9	54.0	56.1
Spatial-MLLM-4B [61]	38.1	49.3	43.7	63.7	58.9	61.3	52.5	44.0
SpaceMind [72]	66.3	53.2	<u>59.7</u>	<u>76.2</u>	<u>70.5</u>	<u>73.8</u>	<u>67.3</u>	–
EgoMind [9]	–	–	–	–	–	–	55.0	58.0
SpaceMind++ (Ours)	<u>56.7</u>	65.6	61.1	76.5	82.3	78.9	70.0	61.0

SI are already highly competitive spatial reasoning models, SpaceMind++ further improves several key subcategories that directly reflect the benefits of allocentric cognitive map construction.

Specifically, SpaceMind++ improves relative distance estimation from 67.7 to 73.5 and appearance ordering from 70.7 to 84.1. Relative distance estimation requires metric grounding between objects in 3D space, while appearance ordering further requires preserving temporal object events and spatial relationships across changing viewpoints. We also observe competitive performance on object count, room size, and relative direction estimation. Overall, the performance suggests that SpaceMind++ is most effective when spatial reasoning requires persistent object-level memory and metric consistency across viewpoints, which are precisely the capabilities targeted by the voxelized cognitive map.

5.2 Generalization to Spatial Reasoning Benchmarks

SPBench. SPBench evaluates spatial reasoning under both single-image and multi-view (eight images) settings[30]. As shown in Table 2, SpaceMind++ maintains competitive performance on the single-image subset while achieving a substantial improvement on the multi-view subset. Specifically, SpaceMind++ obtains 61.1 on SPBench-SI and 78.9 on SPBench-MV, leading to a strong overall score. The large gain on SPBench-MV is particularly consistent with our design motivation: by projecting frame-level observations into a shared 3D cognitive map, SpaceMind++ can better aggregate cross-view evidence and maintain object relationships across viewpoints. This suggests that the learned spatial representation generalizes to out-of-domain multi-view spatial QA.

SITE-Bench. SITE-Bench evaluates spatial intelligence in a multiple-choice VQA format across single-image, multi-image, and video inputs[57]. Since its image subset mostly contains only 1–5 input frames, such short visual contexts provide limited cross-view evidence for constructing a reliable cognitive map. We only report the video-only result under the EgoMind-style average metric as an auxiliary generalization reference and do not claim full SITE-Bench superiority. As shown in Table 2, SpaceMind++ achieves competitive performance on SITE-Bench.

SPAR-Bench. SPAR-Bench provides a difficulty-stratified evaluation of spatial understanding[70]. Here, we focus on the high-level split, which emphasizes multi-object relational reasoning and spatial imagination across views. We omit the low- and medium-level splits from the main table because they are dominated by direct depth, distance, and view-alignment perception, while our method is primarily designed to improve persistent spatial representation and cross-view relational reasoning. As shown in Table 3, SpaceMind++ achieves the best average performance among open-source models, with clear advantages on multi-view object-relation and spatial-imagination tasks. These tasks require cross-view object association and hypothetical-view reasoning, where our voxelized cognitive map provides a stable 3D reference frame for object identities and spatial relations.

Table 3: Generalization evaluation on SPAR-Bench high-level tasks. SpaceMind++ achieves the best average performance, with strong results on multi-view (MV) object-relation (ObjRel) and spatial-imagination (Splmag) tasks, highlighting its advantage in cross-view spatial consistency.

Methods	High Avg.	Dist OO	Dist OO-MV	ObjRel OC-MV	ObjRel OO	ObjRel OO-MV	Splmag OC	Splmag OC-MV	Splmag OO	Splmag OO-MV
<i>Closed-source Models</i>										
GPT-4o [40]	43.80	65.00	64.88	44.75	50.82	43.21	29.84	32.56	27.81	35.29
GPT-4.1 [39]	42.93	71.76	67.26	46.25	54.95	41.00	30.38	29.65	20.20	24.93
Doubao-1.5-vision-pro [4]	49.49	74.71	69.64	35.75	70.33	47.65	34.95	33.14	35.76	42.86
<i>Open-source Models</i>										
InternVL2.5-38B [7]	44.13	69.12	66.67	43.75	64.29	37.67	25.27	31.98	31.79	26.61
Qwen2.5-VL-72B [3]	43.80	58.82	61.90	40.75	53.57	45.98	26.88	35.17	34.11	36.97
LLaVA-v1.6-7B [33]	20.18	51.76	7.74	6.25	32.14	6.37	39.52	10.47	21.52	5.88
SpaceR-7B [41]	45.61	62.35	61.61	52.25	51.92	46.81	37.90	36.05	24.83	34.17
SpaceMind++ (Ours)	51.28	39.78	33.00	70.00	48.63	53.46	51.61	53.78	27.15	45.66

5.3 Ablation Studies

We conduct ablation studies on VSI-Bench to examine the effects of the spatial encoder, cognitive-map construction, and coordinate-guided iterative fusion. As shown in Table 4, the spatial-encoder baseline and architecture-ablation groups are trained on an earlier 626K corpus, which does not include the VSI-590K data, while the final SpaceMind++ model is trained on the final 900K corpus. The architecture ablations use an InternVL3-8B and InternVL3.5-8B backbone. Therefore, this table is intended to reveal component-level trends rather than provide a strictly controlled comparison under identical training settings.

Adding VGGT-based spatial features improves the InternVL3-8B SFT baseline from 63.7 to 64.6, indicating that feed-forward geometry provides useful but limited spatial cues. DIF denotes the non-coordinate-guided variant of our CDIF module. The architecture ablation further shows that introducing a cognitive map into DIF improves the average score from 66.3 to 68.9, suggesting that organizing visual observations into a structured map is beneficial for spatial reasoning. The full SpaceMind++ model achieves the best overall performance, reaching 73.2 with CDIF. This gain should be attributed to both the proposed coordinate-guided architecture, where coordinate embeddings and 3D RoPE explicitly guide information transfer during map reasoning and map-to-visual reading, and the richer 900K training corpus, which includes VSI-590K.

Table 4: Ablation study on VSI-Bench.

Methods	Avg.	Num.	MCQ
<i>Spatial-Encoder Baseline</i>			
InternVL3-8B SFT (626K)	63.7	65.5	61.9
InternVL3-8B + VGGT (626K)	64.6	66.2	63.0
<i>Model Architecture</i>			
InternVL3.5-8B + DIF (626K)	66.3	67.5	65.0
InternVL3.5-8B + CogMap + DIF (626K)	68.9	69.5	68.2
SpaceMind++ (900K)	73.2	72.9	73.9

6 Conclusion

SpaceMind++ achieves state-of-the-art performance on VSI-Bench and generalizes well to SPBench, SITE-Bench, and SPAR-Bench, with clear gains on tasks requiring object-level memory, metric consistency, and cross-view integration. These improvements come from treating 3D geometry not as an auxiliary feature, but as an organizing structure: SpaceMind++ consolidates fragmented egocentric observations into a persistent voxelized allocentric cognitive map and transfers spatial knowledge back to visual tokens through Coordinate-Guided Deep Iterative Fusion. Overall, our results highlight cognitive map construction as a promising direction for spatially grounded video MLLMs.

Limitations and Future Work. SpaceMind++ has several limitations. First, its cognitive map depends on the quality of the feed-forward spatial encoder; inaccurate point maps, incomplete geometry, or sparse observations can weaken the resulting spatial representation. Second, although voxelization reduces token redundancy, map reasoning and map-to-visual fusion introduce extra computation, and a fixed voxel budget may discard fine-grained details in large scenes. Future work could explore uncertainty-aware map construction, adaptive or hierarchical voxel allocation, and extensions to dynamic scenes, interactive embodied agents, and long-horizon spatial memory.

References

- [1] Jean-Baptiste Alayrac, Jeff Donahue, Pauline Luc, Antoine Miech, Iain Barr, Yana Hasson, Karel Lenc, Arthur Mensch, Katherine Millican, Malcolm Reynolds, and others. Flamingo: A visual language model for few-shot learning. In *Advances in Neural Information Processing Systems*, 2022.
- [2] Jinze Bai, Shuai Bai, Shusheng Yang, Shijie Wang, Sinan Tan, Peng Wang, Junyang Lin, Chang Zhou, and Jingren Zhou. Qwen-VL: A frontier large vision-language model with versatile abilities. *arXiv*, abs/2308.12966, 2023.
- [3] Shuai Bai, Keqin Chen, Xuejing Liu, Jialin Wang, Wenbin Ge, Sibao Song, Kai Dang, Peng Wang, and others. Qwen2.5-VL technical report. *arXiv*, abs/2502.13923, 2025.
- [4] ByteDance Seed et al. Seed1.5-VL technical report. *arXiv*, abs/2505.07062, 2025.
- [5] Wenxiao Cai, Iaroslav Ponomarenko, Jianhao Yuan, Xiaoqi Li, Wankou Yang, Hao Dong, and Bo Zhao. SpatialBot: Precise spatial understanding with vision language models. In *IEEE International Conference on Robotics and Automation*, 2025.
- [6] Zhongang Cai, Ruisi Wang, Chenyang Gu, Fanyi Pu, Junxiang Xu, Yubo Wang, Wanqi Yin, Zhitao Yang, Chen Wei, Qingping Sun, Tongxi Zhou, Jiaqi Li, Hui En Pang, Oscar Qian, Yukun Wei, Zhiqian Lin, Xuanke Shi, Kewang Deng, Xiaoyang Han, Zukai Chen, Xiangyu Fan, Hanming Deng, Lewei Lu, Liang Pan, Bo Li, Ziwei Liu, Quan Wang, Dahua Lin, and Lei Yang. Scaling spatial intelligence with multimodal foundation models. *arXiv*, abs/2511.13719, 2025.
- [7] Zhe Chen, Weiyun Wang, Yue Cao, Yangzhou Liu, Zhangwei Gao, Erfei Cui, Jinguo Zhu, Shenglong Ye, Hao Tian, Zhaoyang Liu, Lixin Gu, Xuehui Wang, et al. Expanding performance boundaries of open-source multimodal models with model, data, and test-time scaling. *arXiv*, abs/2412.05271, 2024.
- [8] Zhe Chen, Jiannan Wu, Wenhai Wang, Weijie Su, Guo Chen, Sen Xing, Muyan Zhong, Qinglong Zhang, Xizhou Zhu, Lewei Lu, Bin Li, Ping Luo, Tong Lu, Yu Qiao, and Jifeng Dai. InternVL: Scaling up vision foundation models and aligning for generic visual-linguistic tasks. In *Proceedings of the IEEE/CVF Conference on Computer Vision and Pattern Recognition*, 2024.
- [9] Zhenghao Chen, Huiqun Wang, and Di Huang. EgoMind: Activating spatial cognition through linguistic reasoning in MLLMs. *arXiv*, abs/2604.03318, 2026.
- [10] An-Chieh Cheng, Hongxu Yin, Yang Fu, Qiushan Guo, Ruihan Yang, Jan Kautz, Xiaolong Wang, and Sifei Liu. SpatialRGPT: Grounded spatial reasoning in vision-language models. In *Advances in Neural Information Processing Systems*, 2024.
- [11] Gheorghe Comanici, David Bieber, Mike Schaekermann, Panupong Pasupat, Naveen Sachdeva, Inderjit Dhillon, Michael Blistein, Ori Ram, Dan Zhang, Evan Rosen, et al. Gemini 2.5: Pushing the frontier with advanced reasoning, multimodality, long context, and next generation agentic capabilities. *arXiv*, abs/2507.06261, 2025.
- [12] Russell A. Epstein, Eva Zita Patai, Joshua B. Julian, and Hugo J. Spiers. The cognitive map in humans: Spatial navigation and beyond. *Nature Neuroscience*, 20(11):1504–1513, 2017. doi: 10.1038/nn.4656.
- [13] Zhiwen Fan, Jian Zhang, Renjie Li, Junge Zhang, Runjin Chen, Hezhen Hu, Kevin Wang, Huaizhi Qu, Dilin Wang, Zhicheng Yan, Hongyu Xu, Justin Theiss, Tianlong Chen, Jiachen Li, Zhengzhong Tu, Zhangyang Wang, and Rakesh Ranjan. VLM-3r: Vision-language models augmented with instruction-aligned 3d reconstruction. In *Proceedings of the IEEE/CVF Conference on Computer Vision and Pattern Recognition*, 2026.
- [14] Kaituo Feng, Kaixiong Gong, Bohao Li, Zonghao Guo, Yibing Wang, Tianshuo Peng, Benyou Wang, and Xiangyu Yue. Video-R1: Reinforcing video reasoning in MLLMs. *arXiv*, abs/2503.21776, 2025.

- [15] Qing Feng. Towards visuospatial cognition via hierarchical fusion of semantic and spatial representations. *arXiv*, abs/2505.12363, 2025.
- [16] Rao Fu, Jingyu Liu, Xilun Chen, Yixin Nie, and Wenhan Xiong. Scene-LLM: Extending language model for 3d visual understanding and reasoning. In *Proceedings of the IEEE/CVF Winter Conference on Applications of Computer Vision*, 2025.
- [17] Xiangjun Gao, Zhensong Zhang, Dave Zhenyu Chen, Songcen Xu, Long Quan, Eduardo Pérez-Pellitero, and Youngkyoon Jang. Map2thought: Explicit 3d spatial reasoning via metric cognitive maps. *arXiv*, abs/2601.11442, 2026.
- [18] Melvyn A. Goodale and A. David Milner. Separate visual pathways for perception and action. *Trends in Neurosciences*, 15(1):20–25, 1992. doi: 10.1016/0166-2236(92)90344-8.
- [19] Google DeepMind. Gemini 3 pro: The frontier of vision AI, 2025. Accessed: 2026-03-21.
- [20] Saurabh Gupta, Varun Tolani, James Davidson, Sergey Levine, Rahul Sukthankar, and Jitendra Malik. Cognitive mapping and planning for visual navigation. In *Proceedings of the IEEE Conference on Computer Vision and Pattern Recognition*, pages 2616–2625, 2017.
- [21] Chanyoung Gwak, Yoonwoo Jeong, Byungwoo Jeon, Hyunseok Lee, Jinwoo Shin, and Minsu Cho. Cog3dmap: Multi-view vision-language reasoning with 3d cognitive maps. *arXiv*, abs/2603.23023, 2026.
- [22] Torkel Hafting, Marianne Fyhn, Sturla Molden, May-Britt Moser, and Edvard I. Moser. Microstructure of a spatial map in the entorhinal cortex. *Nature*, 436(7052):801–806, 2005. doi: 10.1038/nature03721.
- [23] Yining Hong, Haoyu Zhen, Peihao Chen, Shuhong Zheng, Yilun Du, Zhenfang Chen, and Chuang Gan. 3d-LLM: Injecting the 3d world into large language models. In *Advances in Neural Information Processing Systems*, 2023.
- [24] J. Edward Hu, Yelong Shen, Phillip Wallis, Zeyuan Allen-Zhu, Yuanzhi Li, Shean Wang, and Weizhu Chen. Lora: Low-rank adaptation of large language models. *ArXiv*, abs/2106.09685, 2021.
- [25] Wenbo Hu, Yining Hong, Yanjun Wang, Leison Gao, Zibu Wei, Xingcheng Yao, Nanyun Peng, Yonatan Bitton, Idan Szpektor, and Kai-Wei Chang. 3d-llm-mem: Long-term spatial-temporal memory for embodied 3d large language model. *arXiv*, abs/2505.22657, 2025.
- [26] Yibin Huang, Wang Xu, Wanyue Zhang, Helu Zhi, Jingjing Huang, Yangbin Xu, Yangang Sun, Conghui Zhu, and Tiejun Zhao. Video2layout: Recall and reconstruct metric-grounded cognitive map for spatial reasoning. *arXiv*, abs/2511.16160, 2025.
- [27] Benjamin Kuipers. The spatial semantic hierarchy. *Artificial Intelligence*, 119(1–2):191–233, 2000.
- [28] Vincent Leroy, Yohann Cabon, and Jerome Revaud. MAST3r: Grounding image matching in 3d. *arXiv*, abs/2406.09756, 2024.
- [29] Bo Li, Yuanhan Zhang, Dong Guo, Renrui Zhang, Feng Li, Hao Zhang, Kaichen Zhang, Peiyuan Li, Yanwei Liu, and Chunyuan Li. LLaVA-OneVision: Easy visual task transfer. *arXiv*, abs/2408.03326, 2024.
- [30] Hongxing Li, Dingming Li, Zixuan Wang, Yuchen Yan, Hang Wu, Wenqi Zhang, Yongliang Shen, Weiming Lu, Jun Xiao, and Yueting Zhuang. SpatialLadder: Progressive training for spatial reasoning in vision-language models. *arXiv*, abs/2510.08531, 2025.
- [31] Junnan Li, Dongxu Li, Silvio Savarese, and Steven C. H. Hoi. BLIP-2: Bootstrapping language-image pre-training with frozen image encoders and large language models. In *International Conference on Machine Learning*, volume 202, pages 19730–19742, 2023.
- [32] Bin Lin, Bin Zhu, Yang Ye, Munan Ning, Peng Jin, and Li Yuan. Video-LLaVA: Learning united visual representation by alignment before projection. *arXiv*, abs/2311.10122, 2024.

- [33] Haotian Liu, Chunyuan Li, Yuheng Li, Bo Li, Yuanhan Zhang, Sheng Shen, and Yong Jae Lee. LLaVA-NeXT: Improved reasoning, OCR, and world knowledge. <https://llava-v1.github.io/blog/2024-01-30-llava-next/>, 2024.
- [34] Ilya Loshchilov and Frank Hutter. Decoupled weight decay regularization. In *International Conference on Learning Representations*, 2019.
- [35] Xiaojian Ma, Silong Yong, Zilong Zheng, Qing Li, Yitao Liang, Song-Chun Zhu, and Siyuan Huang. SQA3d: Situated question answering in 3d scenes. In *International Conference on Learning Representations*, 2023.
- [36] Yongsen Mao, Junhao Zhong, Chuan Fang, Jia Zheng, Rui Tang, Hao Zhu, Ping Tan, and Zihan Zhou. SpatialLM: Training large language models for structured indoor modeling. *arXiv*, abs/2506.07491, 2025.
- [37] Moonshot AI et al. Kimi-VL technical report. *arXiv*, abs/2504.07491, 2025.
- [38] John O’Keefe and Lynn Nadel. *The Hippocampus as a Cognitive Map*. Clarendon Press, Oxford, 1978.
- [39] OpenAI, Josh Achiam, Steven Adler, Sandhini Agarwal, Lama Ahmad, Ilge Akkaya, Florenca Leoni Aleman, Diogo Almeida, Janko Altenschmidt, Sam Altman, et al. GPT-4 technical report. *arXiv*, abs/2303.08774, 2023.
- [40] OpenAI, Aaron Hurst, Adam Lerer, Adam P. Goucher, Adam Perelman, Aditya Ramesh, Aidan Clark, AJ Ostrow, Akila Welihinda, Alan Hayes, et al. GPT-4o system card. *arXiv*, abs/2410.21276, 2024.
- [41] Kun Ouyang, Yuanxin Liu, Haoning Wu, Yi Liu, Hao Zhou, Jie Zhou, Fandong Meng, and Xu Sun. SpaceR: Reinforcing MLLMs in video spatial reasoning. *arXiv*, abs/2504.01805, 2025.
- [42] Alec Radford, Jong Wook Kim, Chris Hallacy, Aditya Ramesh, Gabriel Goh, Sandhini Agarwal, Girish Sastry, Amanda Askell, Pamela Mishkin, Jack Clark, Gretchen Krueger, and Ilya Sutskever. Learning transferable visual models from natural language supervision. In *International Conference on Machine Learning*, pages 8748–8763, 2021.
- [43] Edmund T. Rolls. Spatial view cells and the representation of place in the primate hippocampus. *Hippocampus*, 9(4):467–480, 1999.
- [44] Edmund T. Rolls, Richard G. Robertson, and Philippe Georges-Francois. Spatial view cells in the primate hippocampus. *European Journal of Neuroscience*, 9(8):1789–1794, 1997. doi: 10.1111/j.1460-9568.1997.tb01538.x.
- [45] Shouwei Ruan, Liyuan Wang, Caixin Kang, Qihui Zhu, Songming Liu, Xingxing Wei, and Hang Su. From reactive to cognitive: Brain-inspired spatial intelligence for embodied agents. *arXiv*, 2025.
- [46] Johannes L. Schönberger and Jan-Michael Frahm. Structure-from-motion revisited. In *Proceedings of the IEEE Conference on Computer Vision and Pattern Recognition*, pages 4104–4113, 2016.
- [47] Johannes L. Schönberger, Enliang Zheng, Marc Pollefeys, and Jan-Michael Frahm. Pixelwise view selection for unstructured multi-view stereo. In *European Conference on Computer Vision*, pages 501–518, 2016.
- [48] Aman Singh et al. OpenAI GPT-5 system card. *arXiv*, abs/2601.03267, 2026.
- [49] Ilias Stogiannidis, Steven McDonagh, and Sotirios A. Tsafaris. Mind the gap: Benchmarking spatial reasoning in vision-language models. *arXiv*, abs/2503.19707, 2025.
- [50] Jianlin Su, Yu Lu, Shengfeng Pan, Ahmed Murtadha, Bo Wen, and Yunfeng Liu. RoFormer: Enhanced transformer with rotary position embedding. *arXiv*, abs/2104.09864, 2021. doi: 10.48550/arXiv.2104.09864.

- [51] Edward C. Tolman. Cognitive maps in rats and men. *Psychological Review*, 55(4):189–208, 1948. doi: 10.1037/h0061626.
- [52] Leslie G. Ungerleider and Mortimer Mishkin. Two cortical visual systems. In David J. Ingle, Melvyn A. Goodale, and Richard J. W. Mansfield, editors, *Analysis of Visual Behavior*, pages 549–586. MIT Press, Cambridge, MA, 1982.
- [53] Fangjinhua Wang, Silvano Galliani, Christoph Vogel, Pablo Speciale, and Marc Pollefeys. PatchmatchNet: Learned multi-view patchmatch stereo. In *Proceedings of the IEEE/CVF Conference on Computer Vision and Pattern Recognition*, pages 14194–14203, 2021.
- [54] Jianyuan Wang, Minghao Chen, Nikita Karaev, Andrea Vedaldi, Christian Rupprecht, and David Novotný. VGGT: Visual geometry grounded transformer. In *Proceedings of the IEEE/CVF Conference on Computer Vision and Pattern Recognition*, pages 5294–5306, 2025.
- [55] Qianqian Wang, Yifei Zhang, Aleksander Holynski, Alexei A. Efros, and Angjoo Kanazawa. CUT3r: Continuous 3d perception model with persistent state. *arXiv*, abs/2501.12387, 2025.
- [56] Shuzhe Wang, Vincent Leroy, Yohann Cabon, Boris Chidlovskii, and Jerome Revaud. DUST3r: Geometric 3d vision made easy. In *Proceedings of the IEEE/CVF Conference on Computer Vision and Pattern Recognition*, pages 20697–20709, 2024.
- [57] Wenqi Wang, Reuben Tan, Pengyue Zhu, Jianwei Yang, Zhengyuan Yang, Lijuan Wang, Andrey Kolobov, Jianfeng Gao, and Boqing Gong. SITE: Towards spatial intelligence thorough evaluation. In *Proceedings of the IEEE/CVF International Conference on Computer Vision*, 2025.
- [58] James C. R. Whittington, Timothy H. Muller, Shirley Mark, Guifen Chen, Caswell Barry, Neil Burgess, and Timothy E. J. Behrens. The tolman-eichenbaum machine: Unifying space and relational memory through generalization in the hippocampal formation. *Cell*, 183(5): 1249–1263, 2020. doi: 10.1016/j.cell.2020.10.024.
- [59] James C. R. Whittington, Joseph Warren, and Timothy E. J. Behrens. Relating transformers to models and neural representations of the hippocampal formation. *arXiv*, abs/2112.04035, 2021.
- [60] James C. R. Whittington, David McCaffary, Jacob J. W. Bakermans, and Timothy E. J. Behrens. How to build a cognitive map: Insights from models of the hippocampal formation. *Nature Neuroscience*, 25(10):1257–1272, 2022. doi: 10.1038/s41593-022-01153-y.
- [61] Diankun Wu, Fangfu Liu, Yi-Hsin Hung, and Yueqi Duan. Spatial-MLLM: Boosting MLLM capabilities in visual-based spatial intelligence. In *Advances in Neural Information Processing Systems*, 2025.
- [62] Junfei Wu, Jian Guan, Kaituo Feng, Qiang Liu, Shu Wu, Liang Wang, Wei Wu, and Tieniu Tan. Reinforcing spatial reasoning in vision-language models with interwoven thinking and visual drawing. *arXiv*, abs/2506.09965, 2025.
- [63] xAI. Grok 4 model card. <https://data.x.ai/2025-08-20-grok-4-model-card.pdf>, 2025. Accessed: 2026-05-06.
- [64] An Yang, Anfeng Li, Baosong Yang, Beichen Zhang, Binyuan Hui, Bo Zheng, Bowen Yu, Chang Gao, Chengen Huang, Chenxu Lv, Chujie Zheng, Dayiheng Liu, Fan Zhou, and others. Qwen3 technical report. *arXiv*, abs/2505.09388, 2025.
- [65] Jihan Yang, Shusheng Yang, Anjali W. Gupta, Rilyn Han, Li Fei-Fei, and Saining Xie. Thinking in space: How multimodal large language models see, remember, and recall spaces. *arXiv*, abs/2412.14171, 2024.
- [66] Rui Yang, Ziyu Zhu, Yanwei Li, Jingjia Huang, Shen Yan, Siyuan Zhou, Zhe Liu, Xiangtai Li, Shuangye Li, Wenqian Wang, Yi Lin, and Hengshuang Zhao. Visual spatial tuning. *arXiv*, abs/2511.05491, 2025.
- [67] Shusheng Yang, Jihan Yang, Pinzhi Huang, Ellis Brown, Zihao Yang, Yue Yu, Shengbang Tong, Zihan Zheng, Yifan Xu, Muhan Wang, Daohan Lu, Rob Fergus, Yann LeCun, Li Fei-Fei, and Saining Xie. Cambrian-s: Towards spatial supersensing in video. *arXiv*, abs/2511.04670, 2025.

- [68] Yao Yao, Zixin Luo, Shiwei Li, Tian Fang, and Long Quan. MVSNet: Depth inference for unstructured multi-view stereo. In *European Conference on Computer Vision*, pages 767–783, 2018.
- [69] Songsong Yu, Yuxin Chen, Hao Ju, Lianjie Jia, Fuxi Zhang, Shaofei Huang, Yuhan Wu, Rundi Cui, Binghao Ran, Zaibin Zhang, Zhedong Zheng, Zhipeng Zhang, Yifan Wang, Lin Song, Lijun Wang, Yanwei Li, Ying Shan, and Huchuan Lu. How far are VLMs from visual spatial intelligence? a benchmark-driven perspective. *arXiv*, abs/2509.18905, 2025.
- [70] Jiahui Zhang, Yurui Chen, Yanpeng Zhou, Yueming Xu, Ze Huang, Jilin Mei, Junhui Chen, Yu-Jie Yuan, Xinyue Cai, Guowei Huang, Xingyue Quan, Hang Xu, and Li Zhang. From flatland to space: Teaching vision-language models to perceive and reason in 3d. *arXiv*, abs/2503.22976, 2025.
- [71] Pingyue Zhang, Zihan Huang, Yue Wang, Jieyu Zhang, Letian Xue, Zihan Wang, Qineng Wang, Keshigeyan Chandrasegaran, Ruohan Zhang, Yejin Choi, Ranjay Krishna, Jiajun Wu, Li Fei-Fei, and Manling Li. Theory of space: Can foundation models construct spatial beliefs through active exploration? *arXiv*, abs/2602.07055, 2026.
- [72] Ruosen Zhao, Zhikang Zhang, Jialei Xu, Jiahao Chang, Dong Chen, Lingyun Li, Weijian Sun, and Zizhuang Wei. SpaceMind: Camera-guided modality fusion for spatial reasoning in vision-language models. *arXiv*, abs/2511.23075, 2025.
- [73] Enshen Zhou, Jingkun An, Cheng Chi, Yi Han, Shanyu Rong, Chi Zhang, Pengwei Wang, Zhongyuan Wang, Tiejun Huang, Lu Sheng, and Shanghang Zhang. RoboRefer: Towards spatial referring with reasoning in vision-language models for robotics. *arXiv*, abs/2506.04308, 2025.
- [74] Chenming Zhu, Tai Wang, Wenwei Zhang, Jiangmiao Pang, and Xihui Liu. LLaVA-3d: A simple yet effective pathway to empowering LMMs with 3d awareness. In *Proceedings of the IEEE/CVF International Conference on Computer Vision*, 2025.
- [75] Jinguo Zhu, Weiyun Wang, Zhe Chen, Zhaoyang Liu, Shenglong Ye, Lixin Gu, Hao Tian, Yuchen Duan, Weijie Su, Jie Shao, Zhangwei Gao, Erfei Cui, Xuehui Wang, Yue Cao, Yangzhou Liu, et al. InternVL3: Exploring advanced training and test-time recipes for open-source multimodal models. *arXiv*, abs/2504.10479, 2025.